Study on pollination mechanism of Codonopsis pilosula in Gansu

Shaoming SHI (2021212745@nwnu.edu.cn)
Northwest Normal University
Yujie Zhang
Northwest Normal University
Fan Zhao
Northwest Normal University
Xinxin Zhang
Northwest Normal University
Zhiqi Wang
Northwest Normal University
Lujie Yang
Northwest Normal University
Huilin Liu
Northwest Normal University
Pengxia Shi
Northwest Normal University
Hui Zhang
Northwest Normal University https://orcid.org/0000-0002-9065-6956

Research Article

Keywords: Dichogamy, RNA-seq, Self-incompatibility, SLF, S-RNase

Posted Date: July 24th, 2023

DOI: https://doi.org/10.21203/rs.3.rs-3016755/v1

Abstract

Codonopsis pilosula, a renowned traditional Chinese herbal medicine indigenous to the northwest region of China, was investigated to determine its pollination mechanism. Two Gansu cultivars were utilized to conduct a field pollination experiment, wherein pollen viability and stigma acceptability were assessed, and the single flower cycle was observed. The findings confirmed the existence of dichogamy and Secondary Pollen Presentation in *Codonopsis pilosula*. Furthermore, Transcriptome sequencing analysis was conducted, revealing the presence of the *S-RNase* and *SLF*-controlled S-RNase self-incompatibility systems.

1 Introduction

Codonopsis pilosula is the dried roots of *Codonopsis pilosula* (Franch.) Nannf, *Codonopsis pilosula* Nannf. var. modesta (Nannf.) L. T. Shen and *Codonopsis* tangshen Oliv., which are belongs to Campanulaceae (Liao et al. 2017; Xiong et al. 2018; Wang et al. 2022). As a well-known traditional Chinese medicine, *Codonopsis pilosula* has the effect of strength spleed and tonifying lung, nourishing blood and engendering liquid (Chao et al. 2015; Xie et al. 2017; Yang et al. 2020), which is normally used as a replacement for expensive ginseng (Zou et al. 2019; Bai et al. 2022). Secondary pollen presentation is that pollen was released directly from anther to another organ surface (frequently females) to pollinator, which affects reproduction (Ladd and Donaldson 1993; Castro et al. 2008). Dense villous structure on stigma surface and Some of the accessory structures of the style can be used for pollen presentation (Ladd 1994). Secondary Pollen Presentation can be divided into two periods. The first stage is the male stage, when the anther adheres tightly to the stigma, but the stigma does not crack, and this stage lasts for 1–3 days. The second is the female stage, when the pollen is released by anther, and the movement of filaments makes the anther leave the stigma, leading to the self-pollen is exposed and taken away by pollinators. Then the stigma dehination allows the cross-flower pollen to be placed on the inner surface of the stigma (Stephenson et al. 2000). Secondary Pollen Presentation results in a large amount of self-flowering pollen on the stigma, but it is difficult for own pollen of the species to reach the receptive surface of the stigma for pollination. Thus, most of these plants are dichogamy or outcrossing (Ladd 1994). Dichogamy refers to the temporal separation of sexual functions in hermaphrodite plants (Tel-Zur and Keasar 2020). In general, it is an effective floral mechanism used by plants to avoid self-fertilization, but an increasing number of researchers have found that many species of dichogamy are also self-incompatibility (Bai and Zhang 2005). Self-incompatibility (SI) system is one of the most important systems for sexual reproduction in many angiosperm, which can inhibit self-crossing and increase the genetic diversity of plants (Thomas et al. 2006; Hiroi et al. 2013; Chen et al. 2018). There are two types of self-incompatibility (SI) in plants: sporophytic self-incompatibility (SSI) and gametophytic self-incompatibility (GSI) according to how the incompatibility phenotype of the pollen grain is determined (Liu et al. 2018; Claessen et al. 2019). SSI phenotypes were determined by a series of complex alleles at S-locus (Edh et al. 2008; Chen et al. 2020), Gametophytic self-incompatibility (GSI) is controlled by a complex S locus containing the pistil determinant *S-RNase* and pollen determinant

SFB/SLF (Puerta et al. 2009; Wang et al. 2012). GSI is further divided into SI of papaveraceae and SI of *S-RNase* in Rosaceae, Solanaceae and Scrophulariaceae (Miller and Kostyun 2011).

Codonopsis pilosula is classified in the Campanulaceae family and codonopsis genus (Nam et al. 2023). Whether there is a self-incompatibility system in this species is unknown. Based on artificial field pollination and transcriptome sequencing (RNA-seq), we verified the pollination characteristics of *Codonopsis pilosula* with low self-setting rate, high natural setting rate, dichogamy, secondary pollen presentation, and the possible S genes controlling self-incompatibility in *Codonopsis pilosula* were mined. Revealing the molecular mechanism of self-incompatibility can provide a new idea for further research on self-incompatibility in platycodon plants.

2 Material and methods

2.1 Plant materials

The seeds of *C.pilosula* No. 1 ('We1') and *C.pilosula* No. 3 ('We3') grown in Weiyuan County, Dingxi City were germinated in laboratory and transplanted to the Experimental Park of Northwest Normal University. ' We3 ' was produced by ' We1 ' radiation mutagenesis breeding (Su 2012; Wang and Song 2015). An annual *C.pilosula var. Modesta* ('Wn') growing in Wenxian County of Longnan City was transplanted into the Experimental Park of Northwest Normal University. Female, male, petal and leave of 'We1-1', 'We1-2', 'We1-6', 'Wn2', 'Wn3', 'Wn5' plants were collected at bud stage, which was quickly frozen in liquid nitrogen, and then stored with dry ice and sent to Beijing Nohe Zhiyuan Technology Co., Ltd. for RNA extraction and related sequencing.

2.2 Natural pollination

During the flowering period, 20 flowers with the same growth condition were selected and marked with labels, and the seed setting rate was counted after the seeds were mature.

2.3 Stigma dehiscent stage pollination

Six flowers were chosen from a specific section of the designated plant for the purpose of being emasculated and bagged prior to flowering. Following stigma dehiscence, the flowers were subsequently pollinated. Pollen was obtained from either the same or different flowers that had released pollen on the day of flowering.

2.4 Pollination during different flowering cycles

A total of 50 flowers were selected from the same part of the plant two days before flowering, and 5 flowers were de-pollinated every day. After pollination, they were bagged for self-pollination, and the pollen was all selected from the pollen released by the flowers of the same plant on the day of flowering.

2.5 Observation of single flowering stage of Codonopsis pilosula

Three flowers of 'We3' plants two days before flowering were selected for hanging and marking, and photos were taken from 8:00 to 9:00 every morning to record the status of stigma and anther until the 7th day after flowering.

2.6 Determination of pollen viability

Acetic magenta method (Yu et al. 2013).

2.7 Determination of pollen germination rate

Anthers were collected from 2 days before flowering to 7 days after flowering (-2 to 5) at the full flowering stage (July to August) and stored in a 1.5 mL centrifuge tube in a seed storage closet at 4℃. The sucrose solution was set at 5 concentrations of 2%, 5%, 8%, 10% and 15%, and counted once every 1 h for 6 h to investigate the optimal sucrose solution and germination time of *Codonopsis pilosula* pollen.

2.8 Determination of stigma acceptability

Stigma receptivity was determined using the benzidine-hydrogen peroxide method (Duan et al. 2019; Gong et al. 2021). The flowers were collected from 2 days before flowering to 7 days after flowering, and the stigma was removed and immersed in a concave slide containing the reaction liquid (benzidine: hydrogen peroxide: water = 4:11:12). If the stigma were permeable, the surrounding stigma would appear blue and a large number of bubbles would appear. The receptivity of the stigma is judged by the depth of dyeing, the speed of bubble formation and the number of bubbles.

2.9 Microscopic observation of pollen tube growth

12 flowers of 'We' plant with the same growth state were selected, castrated and bagged. Pollination was pollinated on the day of complete stigma dehiscence (the third day after flowering), with 6 outcrosses and 6 selfcrosses. 24 hours after pollination, the stigma and style of the flowers were completely removed and placed in the Carnot fixative. The style fixed for 24 hours and rehydrated with 80%, 50%, 30% ethanol and ddH_2O. The samples were softened in 8M NaOH solution for 24 h and rinsed 3 times with ddH_2O (Sogo and Tobe 2006). The samples were transferred to aniline blue dye solution for dark staining overnight (Regan and Moffatt 1990). After complete staining, the style and stigma were observed under a fluorescence microscope.

2.10 Sequencing and Raw Data Processing

Using the Illumina high-throughput sequencing of cDNA library sequencing platform get a lot of high quality reads, referred to as the original data (raw data) (Luff et al. 2019). The original data obtained were evaluated and cut by fastqc and trimmomatic, and the splice, sample identification sequence, low-quality Reads and Reads with more N bases were removed to obtain high-quality Clean reads (Zeng et al. 2019). Software Trinity was used to assemble the obtained Clean reads (Grabherr et al. 2011). After assembly, the script perl 5.22 was used to deredundant and cluster the assembled transcripts, and the unigene database of this species was obtained. The transcriptome sequencing library was further evaluated for

quality (Gu et al. 2017). After qualified evaluation, a series of analysis were carried out for expression level and gene structure.

2.11 Gene expression analysis

Reads sequenced were compared with Unigene library using Bowtie1.3.0 (Langmead et al. 2009). According to the comparison results, expression level was estimated using RSEM 1.2.19 software (Li and Dewey 2011), and the FPKM value was used to represent the expression abundance of corresponding Unigene.

2.12 HMMER search

Hmmer 3.0 (http://www.hmmer.org/) is an application package that uses a statistical Model or Hidden Markov Model (HMM) to search for gene sequences (Eddy 2008). HMM search was conducted on the protein data in the ' We 'transcriptome, and the expected value (E value) was set to be less than 10 − 5 to obtain the candidate sporulation self-incompatibility factors SRK and SCR in ' We ', Self-incompatibility factors pS and sS of papiferae type and self-incompatibility factors T2 nuclease and *SLF/ SLFL/FBK* of S-RNase type.

2.13 Blast search

The candidate T2 nucleases and *SLF/SLFL/FBK* obtained by HMMER search were used as queries to perform TBLASTN search on the Unigene of ' Wn ' and the genome of *Radix Codonopsis Lanceolatae* and *Platycodon grandiflorus.*, and then get their candidate *S-RNase* and *SLF/SLFL/FBK* fragment. The Fgenesh tool (http://linux1.softberry.com/berry.phtml?topic= fgenesh&group = programs&subgroup = gfind) in Softberry website was further used to predict genes.

2.14 Phylogenetic tree construction, protein structure and cell localization analysis

The candidate style S factor and pollen S factor were compared with the identified style S factor and pollen S factor in Solanaceae, Rosaceae and Scrophulariaceae by muscle (Edgar 2004) of MEGA7.0 (https://www.megasoftware.net/) (Kumar et al. 2016). The phylogenetic tree was constructed by Neighbor-Joining method and the Bootstrap value was set to 1000 (Stamatakis 2014).

The number, molecular weight, theoretical isoelectric point, hydrophobicity and other physicochemical properties of amino acids were predicted and analyzed by using Protparam (https://web.expasy.org/protparam/), an online tool provided by ExPaSy (Chen and Liu 2013). The online tool PSORT (https://psort.hgc.jp/) was used for subcellular localization of pollen S factor and style S factor (Meinken et al. 2014). The secondary structure of pollen S factor and style S factor was predicted by online SOPMA program (Chen and Liu 2013).

2.15 RT-PCR and sequencing

To ensure the accuracy of transcriptome sequencing, the total RNA extracted from the samples was reverse transcribed using TaKaRa reverse transcription Kit PrimeScriptTM II 1st Strand cDNA Synthesis Kit, followed by cDNA as a template. The style S gene and pollen S gene were screened by reverse transcription PCR in 6 tissue 'We1-1', 'We1-2', 'We1-6', 'We3-1', 'We3-2', 'We3-5', Cpactin gene was obtained by blast search of Cpactin gene in Arabidopsis Thaliana (Wang et al. 2019).

Table 1
Primer sequence of RT-PCR

Gene	Primer	Bases 5'→3'	Bases
We66712	66712_F	CCAAAAATGTCGGCATGGGG	20
	66712_R	ACATGTGAGTGAGAGAGCGAG	21
We57191	57191_F	CCTTCATGAAAGATGCCACTCC	22
	57191_R	TCAGCCCCAGAGCTCAGATT	20
Cpactin	ACT_F	GTGGWCGTACMACHGGTATTGTG	23
	ACT_R	AGACCTAACCTMACCKCCAAG	21

3 Results

3.1 Seed setting rate and average number of seeds per fruit of Codonopsis pilosula under different treatments

Continuous pollination at flowering stage and stigma dehysis stage were pollinated on Codonopsis, and compared with natural pollination (Fig. 1).

3.2 Observation of single flowering stage of Codonopsis pilosula

Observation showed that the single flower cycle of *Codonopsis pilosula* lasted for ten days (Fig. 2). (a) The anthers wrap tightly around the stigma two days before flowering. (b) Anthers dehiscent and adhere tightly around stigma the day before flowering. (c) (d) On the day of flowering and one day after flowering, the stigma was not dehiscent, the stigma surface was densely villous, the anthers dried up and contracted, and the pollen was still adhered to the stigma. (e) 2 days after flowering, the stigmas were more flat, and the outer surface of stigmas became smooth. At this time, the adherent pollen on the outer surface was nearly absent. (f) (g) From 3 days after flowering to 4 days after flowering the stigma is completely dehiscent and reverse outward rolled, with the inner surface completely exposed. (h) (i) (j) The stigma and style gradually dried and withered from 5 to 7 days after flowering.

3.3 Pollen viability and germination rate

The pollen activity and germination rate of *Codonopsis pilosula* at different flowering stages were consistent with the flowering cycle of single flower. The pollen activity and germination rate of *Codonopsis pilosula* reached the maximum on the day of flowering and decreased with the increase of time (Fig. 3).

3.4 Stigma acceptability

The stigma receptivity was determined at different flowering stages. Consistent with the observation of the flowering process of single flower, the stigma completely cracked on the 3rd day after flowering, and the stigma receptivity reached its maximum on the 3rd day after flowering (Table 2).

Table 2
Stigma acceptability at different flowering stages

time	-2	-1	0	1	2	3	4	5	6	7
Stigma acceptability	-	-	-	+	+	+++	++	-	-	-

-: Stigma incapacitated; +: Stigma with receptivity; ++: Stigma has stronger acceptability; +++:Stigma has Extremely strong acceptability

3.5 Microscopic observation of pollen tube growth

The results showed that both inbred and outbred pollens could germinate on the surface of stigma after stigma cracking, and pollen tubes grew normally. There was no significant difference in the degree of pollen tube elongation between inbred and outbred, which extended to the lower end of style (Fig. 4).

3.6 RNA-seq sequencing analysis

The transcriptome sequencing data of each sample showed that base error rate of each sample is 0.02% or 0.03%, the GC content is above 42.07% and the percentage of Q20 base and Q30 base were more than 97% and 92%, indicating the transcriptome sequencing data was abundant, accurate and of high quality. After assembling the sequencing data, a total of 11925 'Wn' Unigene and 97838 'We' Unigene were obtained. Unigenes length distribution for transcriptome sequencing reported in Table 3.

Table 3
Unigenes length distribution for transcriptome sequencing

Sequence length (bp)	Number of unigene		Percentage (%)	
	We	Wn	We	Wn
300–500	30407	53390	31.08	44.77
500–1000	30815	36126	31.50	30.29
1000–2000	19625	17178	20.06	14.40
> 2000	16991	12561	17.37	10.54
Total	97838	119255	100	100

3.7 Screening of candidate style S factor and pollen S factor

A total of 107 candidate pollen S factors and 7 candidate style S factors in 'We' (Table 4) and 7 candidate pollen S factors and 1 candidate style S factors in 'Wn' (Table 5) were obtained by hmmer and blast search.

Table 4
Candidate style S factor and pollen S factor of *C.pilosula*

Type of SI	Style factor/Pollen factor	E-value	Number of candidate style factors/pollen factors
SSI	SRK	$< 10^{-5}$	827
	SCR/SP11	$< 10^{-5}$	0
Papaveraceae SI	pS	$< 10^{-5}$	0
	sS	$< 10^{-5}$	14
S-RNase SI	RNase T2	$< 10^{-5}$	7
	SLF/SLFL/FBK	$< 10^{-5}$	107

Table 5
Candidate style *S* genes and pollen *S* genes in *C.pilosula*, *C.pilosula* var. *modesta* and *P. grandiflorus*

Style gene/Pollen gene	E-value	Wn	Cl	Pg
RNase T2	$< 10^{-5}$	1	1	2
SLF/SLFL/FBK	$< 10^{-5}$	37	73	86

3.8 Construction of phylogenetic tree of T2 nuclease candidate proteins

The T2 nuclease gene family can be divided into three types (Igic and Kohn 2001). Class III is the Class III T2 nuclease (S-RNase), Class and Class are the class I T2 nuclease and Class II T2 nuclease, respectively. These three types of nucleases can be clearly divided into three branches on the phylogenetic tree (Fig. 5).

3.9 Phylogenetic tree of FBK/SLFL/SLF candidate proteins

Phylogenetic trees were constructed based on the SLF/SLFL/FBK candidates from *C.pilosula, C.pilosula var.modesta* and *C.lanceolate* and the identified SLF/SLFL/FBK from *Rosids* and *Asterid*, The results

showed that all the sequences could be divided into five main branches (Fig. 6). candidate SLF/SLFL in *C.pilosula*, *C.pilosula var. modesta* are show in Table 6.

Table 6
Screened SLF/SLFL in *C.pilosula*, *C.pilosula* var. *modesta* and *C. lanceolata*

species	sequences
C.pilosula	We47165, We32167, We66712, We47287, We41753, We55668, We4697, We45636, We17833, We17829, We39906, We40717, We57191, We54379, We30592, We16714
C.pilosula var. *modesta*	Wn1, Wn25, Wn33, Wn34, Wn36, Wn14

3.10 Tissue specific expression analysis of S-RNase and SLF

The expression levels of pollen S factor and style S factor mentioned above were analyzed and verified by RT-PCR. The results showed that two style S genes (*We36130* and *We36131*) were highly expressed in the female of *C.pilosula*, two pollen S gene (*We66712* and *We54379*) were specifically expressed in the male of *C.pilosula* (Fig. 7). Other S genes were not tissue-specific expressed (Fig. 8), so they were not the S genes controlling SI in *Codonopsis pilosula*.

3.11 Analysis of Sequencing Results

The S genes *We66712* we sequenced in pollen (We11_66712; We12_66712; We16_66712; We31_66712; We32_66712; We35_66712) was compared with the gene sequences obtained by second-generation transcriptome sequencing (*We66712*) (Fig. 9). The results showed that the sequences were basically consistent, indicating that the transcriptome sequencing sequence was accurate.

3.12 Physicochemical properties of S-RNase and SLF proteins

In this study, it was found that the hydrophobicity values of *SRNase* proteins were all positive, indicating that they were hydrophobic proteins, but the degree of hydrophobicity was different. The hydrophobicity of *SLF* proteins is negative (Table 7), indicating that all of them are hydrophilic proteins, but there are differences in the degree of hydrophilicity.

Table 7
Physical and chemical properties of *SRNase* and *SLF* in *C.pilosula*

Protein	Length/aa	MW/kDa	PI	Hydrophobicity	Instability coefficient	Aliphatic-aa coefficient	Arg + Lys
We36130	698	59675.68	5.12	0.906	54.75	31.23	0
We36131	315	26040.21	5.29	0.926	40.77	37.78	0
We54379	411	47087.31	8.59	-0.142	45.90	87.71	45
We66712	485	56158.08	8.34	-0.067	37.01	90.39	49

3.13 Predictive analysis of secondary structure of S-RNase and SLF

The secondary structure analysis of S-RNase and SLF proteins showed that the secondary structure of *SRNase* and *SLF* in *C.pilosula* mainly consisted of α-helix, β-folding, random curling and extended chain structure, which was similar to the secondary structure of other five identified *S-RNase* and *SLF* proteins.

3.14 Subcellular localization analysis of S-RNase and SLF

The subcellular localization results of *S-RNase* and *SLF* proteins showed that S-RNase in *C.pilosula* was located in extracellular cells, suggesting that the protein might be secreted. SLF proteins were all located in the cytoplasm (Table 8), suggesting that they might be non-secretory proteins. S-RNase is expressed in large amounts in the style and secreted into the Style transport tissue extracellular matrix. In incompatible plants, *S-RNase* enters into the pollen tube and decomposes the RNA in the pollen tube, resulting in the growth disorder of the pollen tube, thus affecting the synthesis of proteins and causing the self-incompatibility reaction (Yu et al. 2019; Zhang and Xue 2019).

Table 8
S-RNase and *SLF* subcellular localization in *C.pilosula*

Protein	Site	Certainty (%)
We36130	extracellular	9.7
We36131	extracellular	11.1
We54379	nucleus	10.8
We66712	chloroplast	3.0

4 Discussion

This study has confirmed that *Codonopsis pilosula* exhibits pollination characteristics that include high natural seed setting and low self-fertilization seed setting. Additionally, the study has confirmed the

presence of dichogamy and pollen secondary presentation pollination characteristics in *Codonopsis pilosula*.

Furthermore, we conducted a transcriptomic analysis to investigate the potential self-incompatibility genes of S nuclease type in *Codonopsis pilosula*. Our findings revealed the identification of four genes, namely *We36130*, *We36131*, *We54379*, and *We66712*. Notably, *We36130* and *We36131* exhibited female-specific expression, while *We54379* and *We66712* demonstrated male-specific expression. Additionally, we successfully detected the specific expressions of *We54379* and *We66712*. The present study involved the prediction of the secondary structure of the genes under investigation, revealing that they predominantly exhibit α-helix, β-folding, random curling, and extended chain structures, akin to the secondary structure of *S-RNase* and *SLF* proteins observed in other organisms. Additionally, subcellular localization analysis indicated that *We36130* and *We36131* are extracellularly located, whereas *We54379* and *We66712* are situated within the cytoplasm, implying their potential involvement in material transport and pollen tube growth. In addition, the exploration of *S-RNase* and *SLF* genes offers a theoretical framework for the genetic enhancement and hybridization techniques of *Codonopsis pilosula*, which are more efficient in terms of time and resource utilization in comparison to conventional selective breeding methods.

Declarations

Acknowledgments

We thank Dingxi Academy of Agricultural Sciences for providing the seeds of 'We'.

Author Contributions

Analysis of pollination data and wrote the paper was contributed by S.S.M. pollination experiments was contributed by Z.Y.J. analysis of transcriptome data was contributed by Z.F. Molecular validation experiments was contributed by Z.X.X. collection and collation of data was contributed by W.Z.Q.,Y.L.J.,L.H.L. and S.P.X.. All authors have read and agreed to the published version of the manuscript.

Funding

This work was funded by Industry Support Plan Project of Gansu Province Higher Education (2022CYZC-14); Lanzhou talent innovation and Entrepreneurship Project (2021-RC-59) and National Natural Science Foundation of China (31060033); Open Fund Project of the State Key Laboratory of Chromosome Engineering, Institute of Genetic Development, Chinese Academy of Sciences (PCCE-KF-2019-06).

Data Availability Statement

The Illumina platforms sequencing data reported in this study are available in the Sequence Read Archive (http:// www.ncbi.nlm.nih.gov/sra) under Accession No. PRJNA974687 and PRJNA974686.

References

1. Bai RB, Wang YP, Fan JM, Zhang JJ, Li W, Zhang Y, Hu FD (2022) Intra-regional classification of Codonopsis Radix produced in Gansu province (China) by multi-elemental analysis and chemometric tools. Sci. Rep 12:1-10.
2. Bai WN, Zhang DY (2005) Sexual interference in cosexual plants and its evolutionary implications. Chinese J. Plant Ecol 29:672.
3. Castro S, Silveira P, Navarro L (2008) How does secondary pollen presentation affect the fitness of Polygala vayredae (Polygalaceae)? Am. J. Bot 95:706-712.
4. Chao CH, Juang SH, Chan HH, Shen DY, Liao YR, Shih HC, Huang CH, Cheng JC, Chen FA, Hung HY (2015) UV-guided isolation of polyynes and polyenes from the roots of Codonopsis pilosula. RSC Adv 5:41324-41331.
5. Chen M, Fan W, Hao B, Zhang W, Yan M, Zhao Y, Liang YL, Liu GZ, Lu YC, Zhang GH (2020) EbARC1, an E3 ubiquitin ligase gene in Erigeron breviscapus, confers self-incompatibility in transgenic Arabidopsis thaliana. Int J Mol Sci 21:1458.
6. Chen NN, Liu JY (2013) Identification and Bioinformatics Analysis of the SnRK2 Gene Family in Apple (Malus×domestica Borkh.). Chinese Agricultural Science Bulletin 29:120-127.
7. Chen QJ, Meng D, Gu ZY, Li W, Yuan H, Duan X, Yang Q, LiY, Li TZ (2018) SLFL genes participate in the ubiquitination and degradation reaction of S-RNase in self-compatible peach. Front Plant Sci 9:227.
8. Claessen H, Keulemans W, Van de Poel B, De Storme N (2019) Finding a compatible partner: Self-incompatibility in European pear (Pyrus communis); molecular control, genetic determination, and impact on fertilization and fruit set. Front Plant Sci 10:407.
9. Duan YF, Li WH, Zheng SY, Sylvester SP, Li YF, Cai FY, Zhang C, Wang XR (2019) Functional androdioecy in the ornamental shrub Osmanthus delavayi (Oleaceae). Plos One 14:e0221898.
10. Eddy SR (2008) A probabilistic model of local sequence alignment that simplifies statistical significance estimation. Plos Comput Biol 4:e1000069.
11. Edgar RC (2004) MUSCLE: multiple sequence alignment with high accuracy and high throughput. Nucleic Acids Res 32:1792-1797.
12. Edh K, Widén B, Ceplitis A (2008) Unequal segregation of SRK alleles at the S locus in Brassica cretica. Genet Res 90:223-228.
13. Gong PC, Song CJ, Liu HY, Li PG, Zhang MS, Zhang JS, Zhang SH, He CY (2021) Physalis floridana CRABS CLAW mediates neofunctionalization of GLOBOSA genes in carpel development. J Exp Bot 72:6882-6903.
14. Grabherr MG, Haas BJ, Yassour M, Levin JZ, Thompson DA, Amit I, Adiconis X, Fan L, Raychowdhury R, Zeng QD (2011) Full-length transcriptome assembly from RNA-Seq data without a reference genome. Nat Biotechnol 29:644-652.

15. Gu CS, Liu LQ, Deng YM, Zhang YX, Wang ZQ, Yuan HY, Huang SZ (2017) De novo characterization of the Iris lactea var. chinensis transcriptome and an analysis of genes under cadmium or lead exposure. Ecotox Environ Safe 144:507-513.
16. Hiroi K, Sone M, Sakazono S, Osaka M, Masuko-Suzuki H, Matsuda T, Suzuki G, Suwabe K, Watanabe M (2013) Time-lapse imaging of self-and cross-pollinations in Brassica rapa. Ann Bot-london 112:115-122.
17. Igic B, Kohn JR (2001) Evolutionary relationships among self-incompatibility RNases. Proc Natl Acad Sci 98:13167-13171.
18. Kumar S, Stecher G, Tamura K (2016) MEGA7: molecular evolutionary genetics analysis version 7.0 for bigger datasets. Mol Biol Evol 33:1870-1874.
19. Ladd PG (1994) Pollen presenters in the flowering plants—form and function. Bot J Linn Socy 115:165-195.
20. Ladd PG, Donaldson JS (1993) Pollen presenters in the South African flora. S Afr J Bot 59:465-477.
21. Langmead B, Trapnell C, Pop M, Salzberg SL (2009) Ultrafast and memory-efficient alignment of short DNA sequences to the human genome. Genome Biol 10:R25.
22. Li B, Dewey CN (2011) RSEM: accurate transcript quantification from RNA-Seq data with or without a reference genome. Bmc Bioinformatics 12:1-16.
23. Liao YY, Zeng LT, Li P, Sun T, Wang C, Li FW, Chen YY, Du B, Yang ZY (2017) Influence of Plant Growth Retardants on Quality of Codonopsis Radix. Molecules 22:1655.
24. Liu W, Pei MS, Zhang AN (2018) Studying on the strictly self-compatibility mechanism of ‘liuyefeitao’peach (Prunus persica L.). Plos One 13:e0200914.
25. Luff J, Mader M, Rowland P, Britton M, Fass J, Yuan H (2019) Viral genome integration of canine papillomavirus 16. PAPILLOMAVIRUS RES 7:88-96.
26. Meinken J, Asch DK, Neizer-Ashun K, Chang GH, Cooper JR CR, Min XJ (2014) FunSecKB2: a fungal protein subcellular location knowledgebase. Comput Mol Biol 4:No7 1-17.
27. Miller JS, Kostyun JL (2011) Functional gametophytic self-incompatibility in a peripheral population of Solanum peruvianum (Solanaceae). Heredity 107:30-39.
28. Nam M, Kim YC, Kim MS (2023) UPLC-QTOF-MS-Based Metabolomics and Antioxidant Capacity of Codonopsis lanceolata from Different Geographical Origins. Foods 12:267.
29. Puerta A, Ushijima K, Koba T, Sassa H (2009) Identification and functional analysis of pistil self-incompatibility factor HT-B of Petunia. J Exp Bot 60:1309-1318.
30. Regan SM, Moffatt BA (1990) Cytochemical analysis of pollen development in wild-type Arabidopsis and a male-sterile mutant. The Plant Cell 2:877-889.
31. Sogo A, Tobe H (2006) Mode of pollen-tube growth in pistils of Myrica rubra (Myricaceae): a comparison with related families. Ann Bot-london 97:71-77.
32. Stamatakis A (2014) RAxML version 8: a tool for phylogenetic analysis and post-analysis of large phylogenies. Bioinformatics 30:1312-1313.

33. Stephenson AG, Good SV, Vogler DW (2000) Interrelationships among inbreeding depression, plasticity in the self-incompatibility system, and the breeding system of Campanula rapunculoides L. (Campanulaceae). Ann Bot-london 85:211-219.
34. Su NN (2012) Study on Seed Testing and Standard for Quality of Codonopsis pilosula(Franch.) Nannf. PUMC
35. Tel-Zur N, Keasar T (2020) Intraspecific Seasonal Variation of Flowering Synchronization in a Heterodichogamous Tree. Plants 9:1509.
36. Thomas SG, Huang SJ, Li ST, Staiger CJ, Franklin-Tong VE (2006) Actin depolymerization is sufficient to induce programmed cell death in self-incompatible pollen. J Cell Biol 174:221-229.
37. Wang SH, Kakui H, Kikuchi S, Koba T, Sassa H (2012) Interhaplotypic heterogeneity and heterochromatic features may contribute to recombination suppression at the S locus in apple (Malus× domestica). J Exp Bot 63:4983-4990.
38. Wang SX, Song ZH (2015) Breeding Report of A New Codonopsis pilosula Variety Weidang 3. GANSU AGRICULTURAL SCIENCE AND TECHNOLOGY 479:11-13.
39. Wang YG, Wang CL, Xue HY, Jin YM, Yang MJ, Leng FF (2022) Comparative analysis of three kinds of extraction kinetic models of crude polysaccharides from codonopsis pilosula and evaluate the characteristics of crude polysaccharides. Biomass Convers Biorefin 19:1-17.
40. Wang YZ, Dai MS, Cai DY (2019) Expression Stability Analysis of Common Internal Reference Genes in Pear Fruit Based on High-throughput Sequencing Molecular plant breeding 17:746-753.
41. Xie M, Yan ZQ, Ren X, Li XZ, Qin B (2017) Codonopilate A, a triterpenyl ester as main autotoxin in cultivated soil of Codonopsis pilosula (Franch.) Nannf. J Agr Food Chem 65:2032-2038.
42. Xiong Y, Zhao QY, Gu LY, Liu CY, Wang C (2018) Shenqi Fuzheng Injection Reverses Cisplatin Resistance through Mitofusin-2-Mediated Cell Cycle Arrest and Apoptosis in A549/DDP Cells. Evid Based Complementary Altern Med 2018:8258246.
43. Yang J, Yang XZ, Li B, Lu XY, Kang JF, Cao XY (2020) Establishment of in vitro culture system for Codonopsis pilosula transgenic hairy roots. 3 Biotech 10:1-8.
44. Yu YM, Zhang M, Lyu YZ, Huang LB, He YP (2013) Pollen viability of three pecan cultivars. Journal of Jiangsu Forestry Science & Technology 40:1-5.
45. Yu ZF, Ma XX, Zeng B (2019) Research Progress on SBP1 Gene of Plant Gametophytic Self-incompatibility. Molecular plant breeding 17:5285-5290.
46. Zeng WY, Sun ZD, Lai ZG, Yang SZ, Chen HZ, Yang XH, Tao JR, Tang XM (2019) Determination of the miRNAs related to bean pyralid larvae resistance in soybean using small RNA and transcriptome sequencing. Int J Mol Sci 20:2966.
47. Zhang YJ, Xue YB (2019) Molecular mechanism of self-incompatibility based on S-nuclease Botanical bulletin 17:130-134.
48. Zou YF, Zhang YY, Fu YP, Inngjerdingen KT, Paulsen BS, Feng B, Zhu ZK, Li LX, Jia RY, Huang C (2019) A polysaccharide isolated from Codonopsis pilosula with immunomodulation effects both in

vitro and in vivo. Molecules 24:3632.

Figures

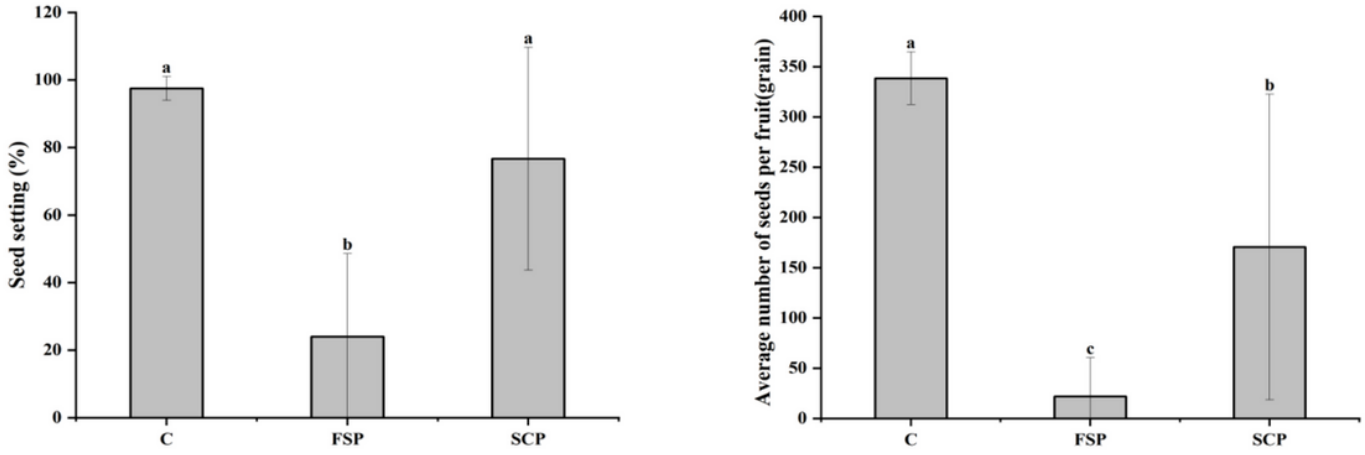

Figure 1

C: natural pollination of *Codonopsis pilosula*; FSP: Pollination during different flowering cycles; SCP: Stigma dehiscent stage pollination. Error bars represent standard deviation. Categories marked by different letters are significantly different ($p<0.01$).

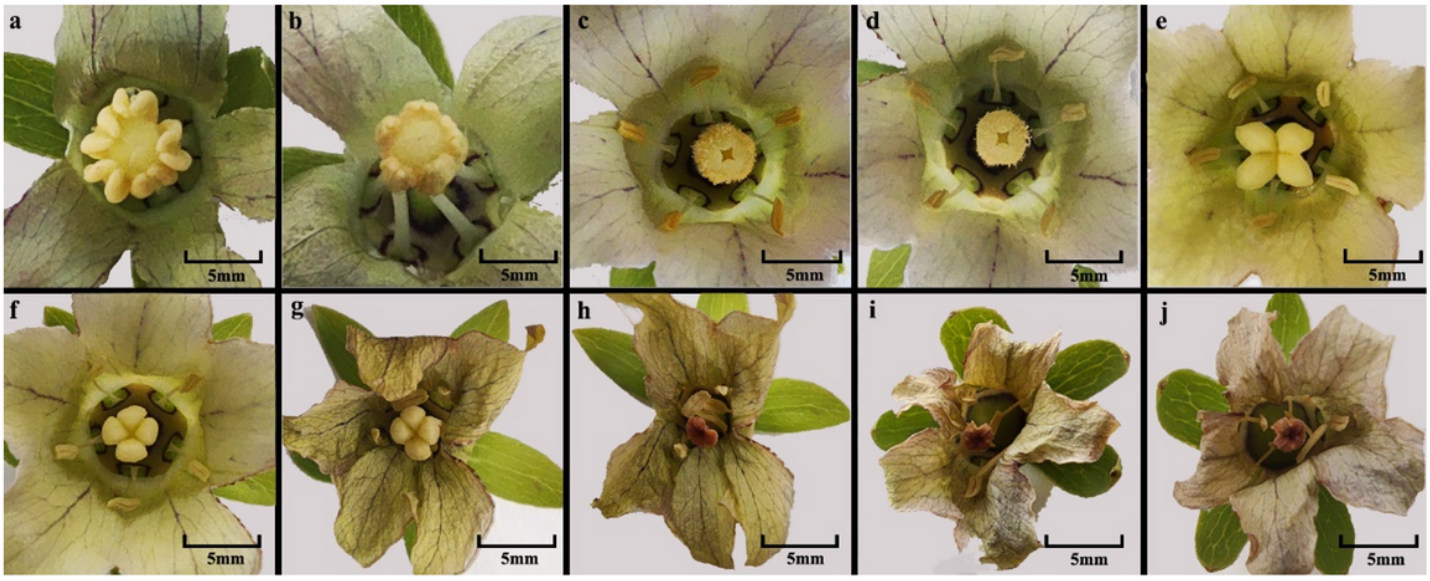

Figure 2

*Codonopsis pilosula*single flower opening process (a) Two days before flowering. (b) One days before flowering. (c): Flowering day. (d) One day after flowering. (e) Two days after flowering. (f) Three days

after flowering. (g) Four days after flowering. (h) Five days after flowering. (i) Six days after flowering. (j) Seven days after flowering

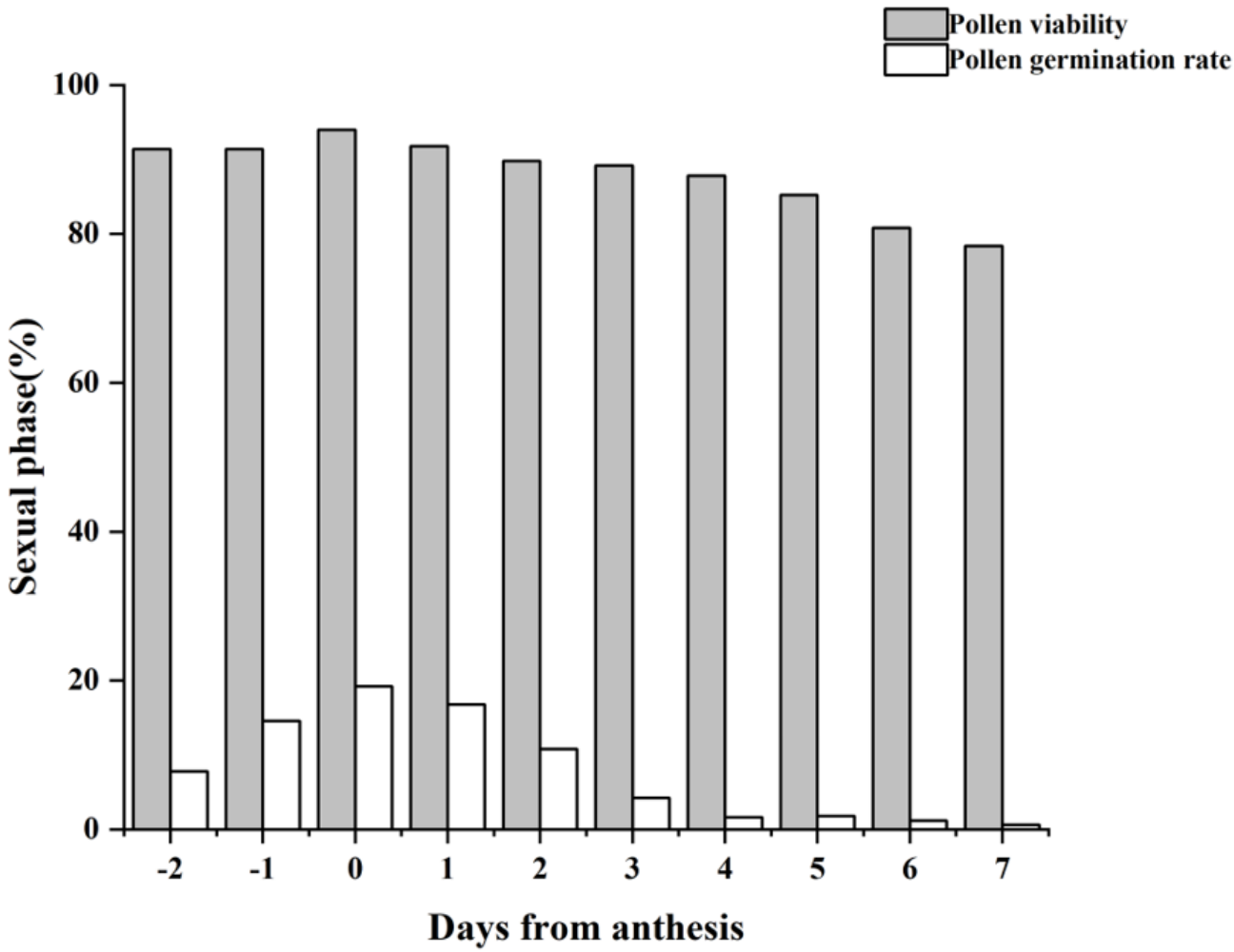

Figure 3

Pollen viability and germination rate changed with the process of flower cycle

-2-7: Two days before flowering to seven days after flowering

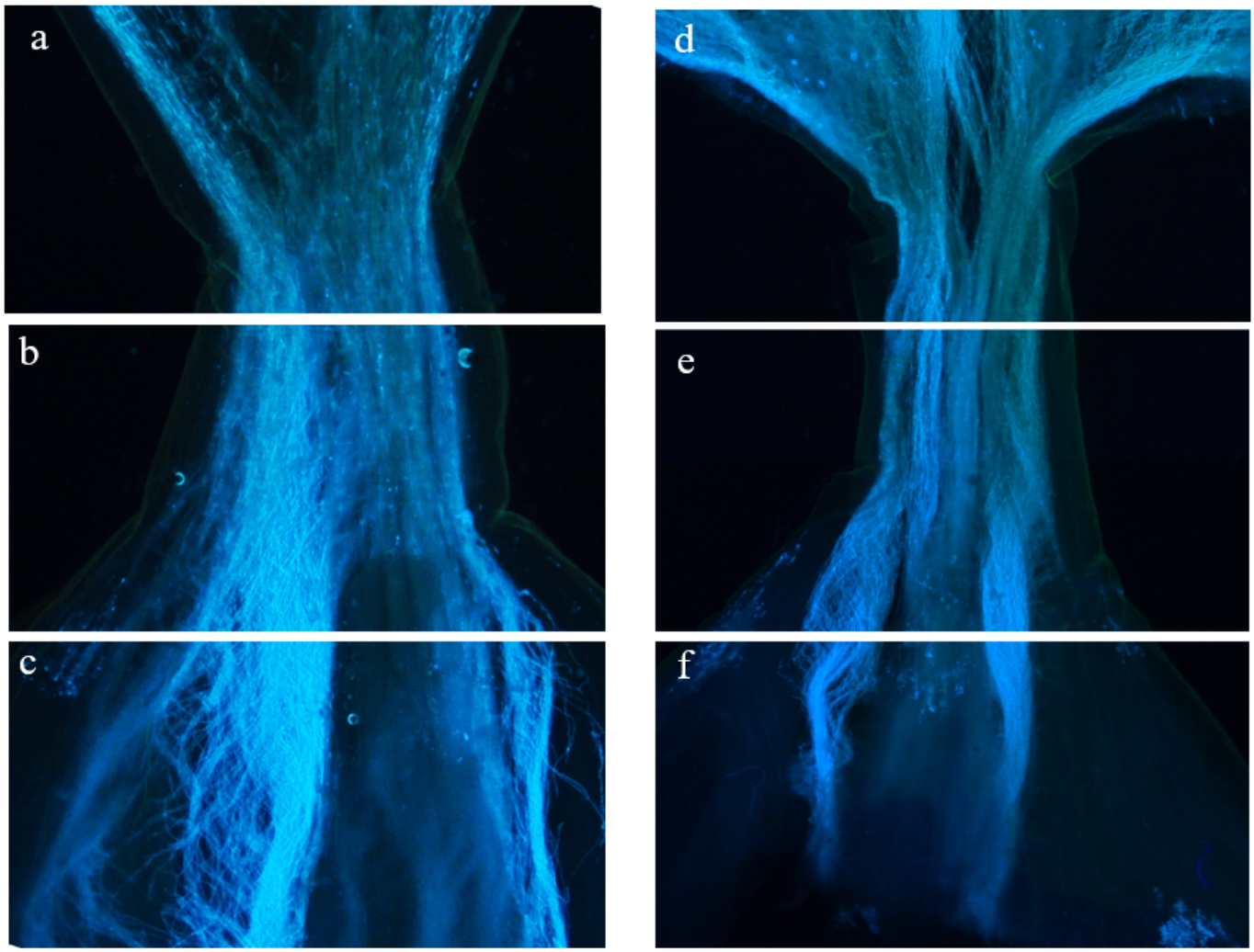

Figure 4

Observation of pollen tube under fluorescence microscope (a), (b) and (c) are self-crossing styles of *Codonopsis pilosula*; (d), (e) and (f) are outcross styles of *Codonopsis pilosula*

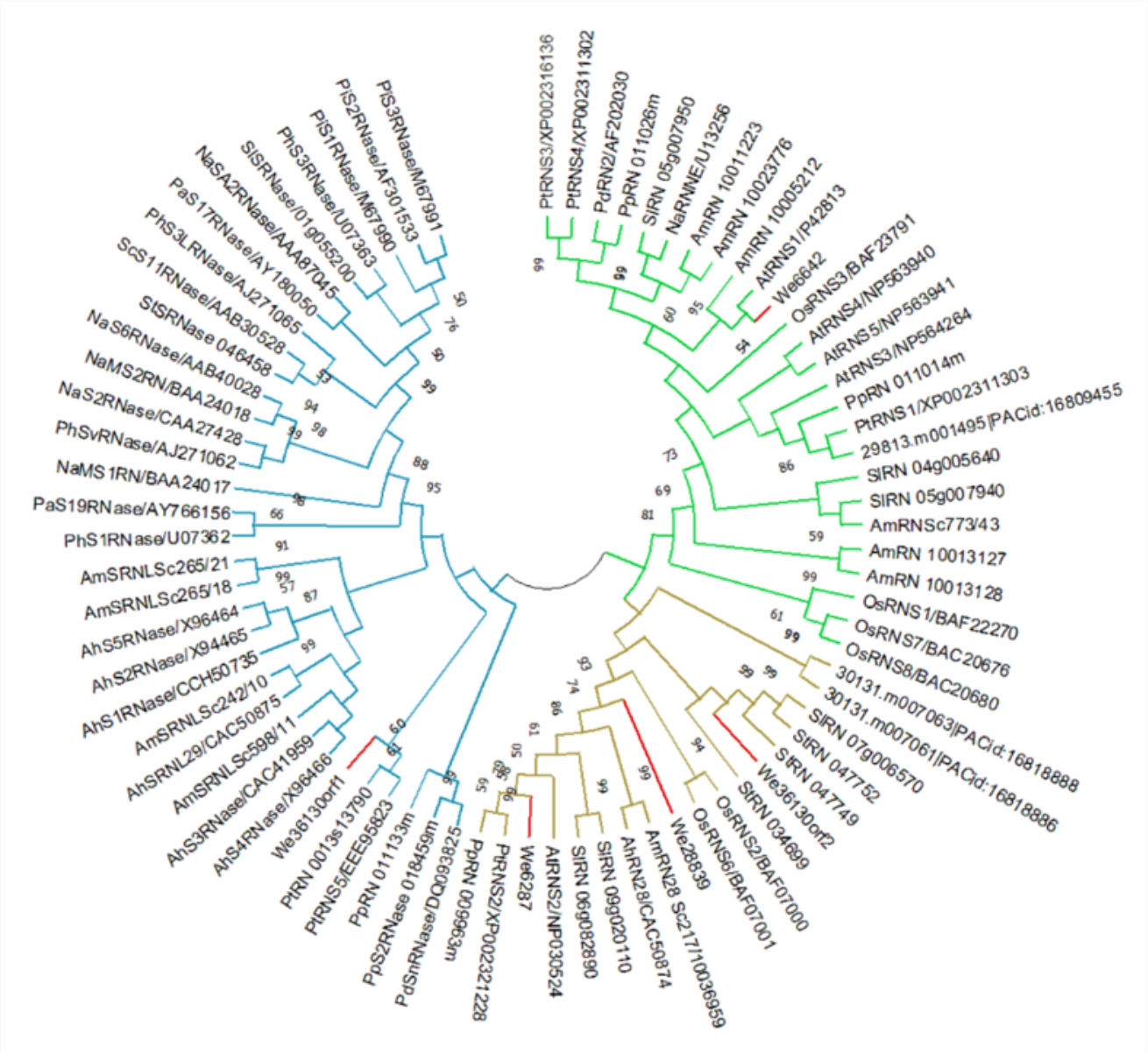

Figure 5

Phylogenetic tree of identified *SRNase* and candidate *SRNase*in *C.pilosula* The green branch is Class I RNase T2. The brown branch is Class II RNase T2. The blue branch is Class III RNase T2. The phylogenetic tree marked in red is RNase T2, screened from the 'We'

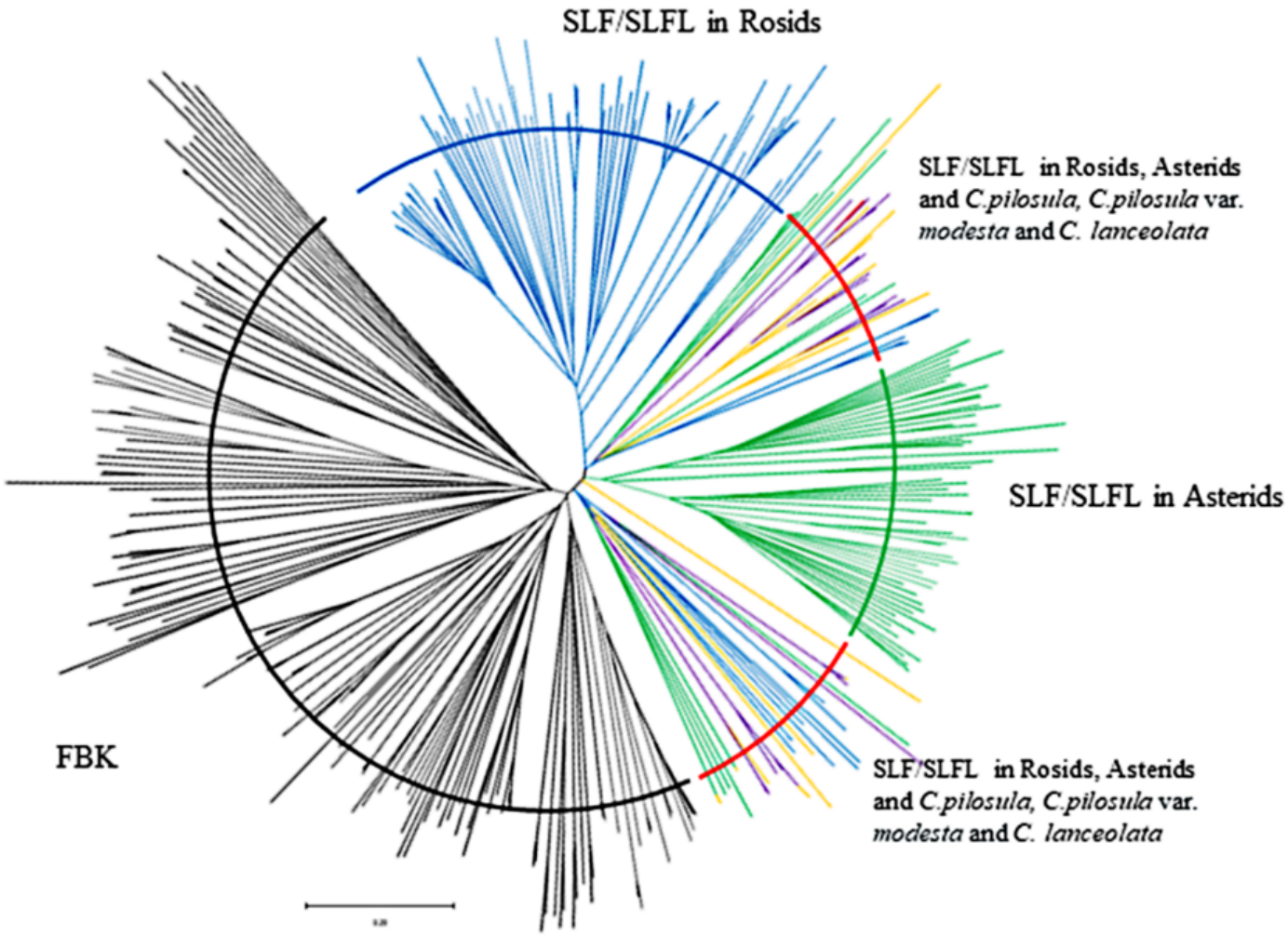

Figure 6

Phylogenetic tree of identified *SLF/SLFL* and candidate *SLF/SLFL/FBK* in *C.pilosula, C.pilosula var. modesta* and C. *lanceolate* The black branch of FBK was identified as non-SLF and non-SLF in *C.pilosula*, *C.pilosula var.modesta* and C. *lanceolate*. The blue indicates the identified SLF/SLFL in the *Rosids*. Those marked in green indicate identified SLFS/SLFLS in *Asterids*. The orange indicates a possible SLF/SLFL in *C.pilosula*. Those marked in red indicate possible SLF/SLFL in *C.pilosula* var. *Modesta*. Those marked in green indicate identified *SLFS/SLFLS* in *C. lanceolate*

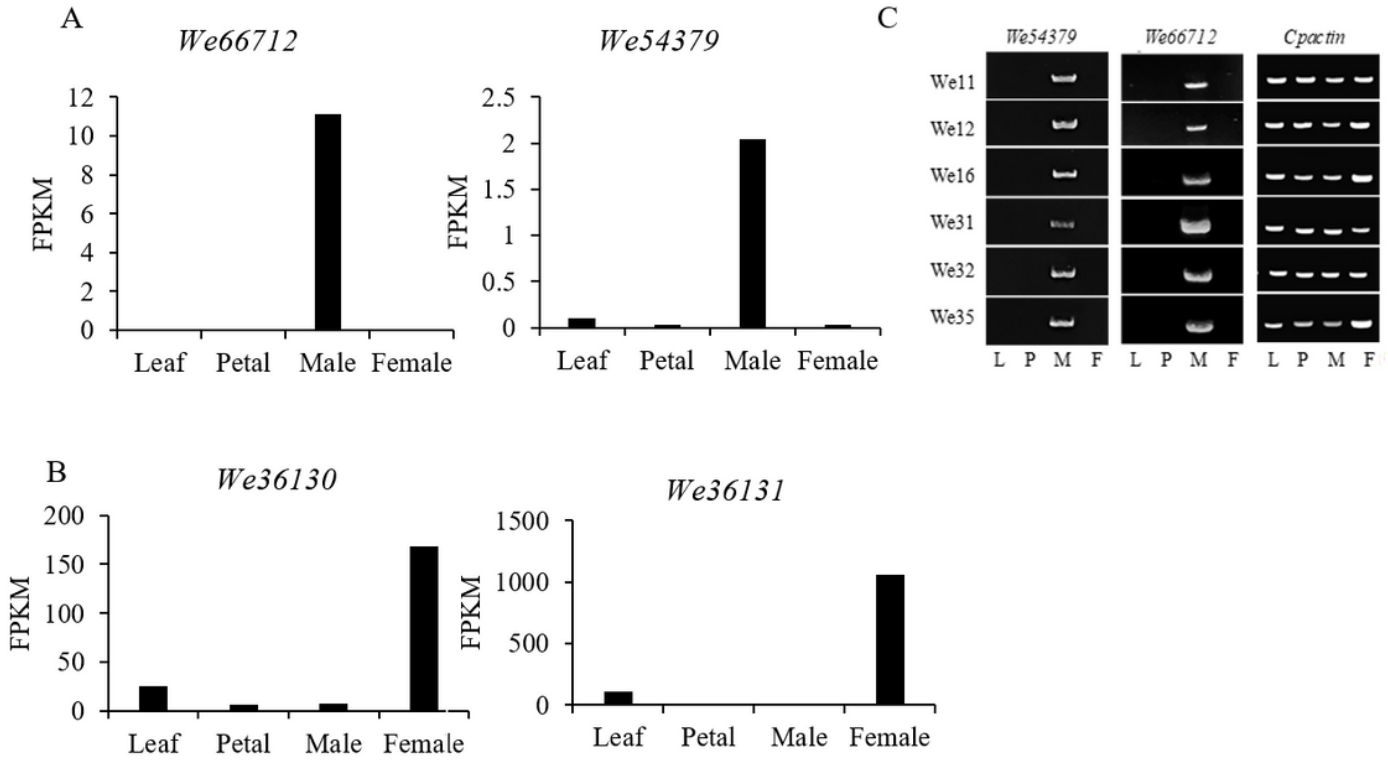

Figure 7

Tissue-specific or highly expressed S-RNase and SLF (A) Tissue-specific expressed pollen S genes. (B) Tissue-specific or highly expressed style S genes. (C) RT-PCR gel electrophoresis of specific or highly expressed S genes. We11, We12, We16, We31, We32, We35 are 6 samples of *C.pilosula* L (Leaf), P (Petal), M (Male), F (Female) are 4 tissues of *C.pilosula*. *Cpactin* is the internal reference gene

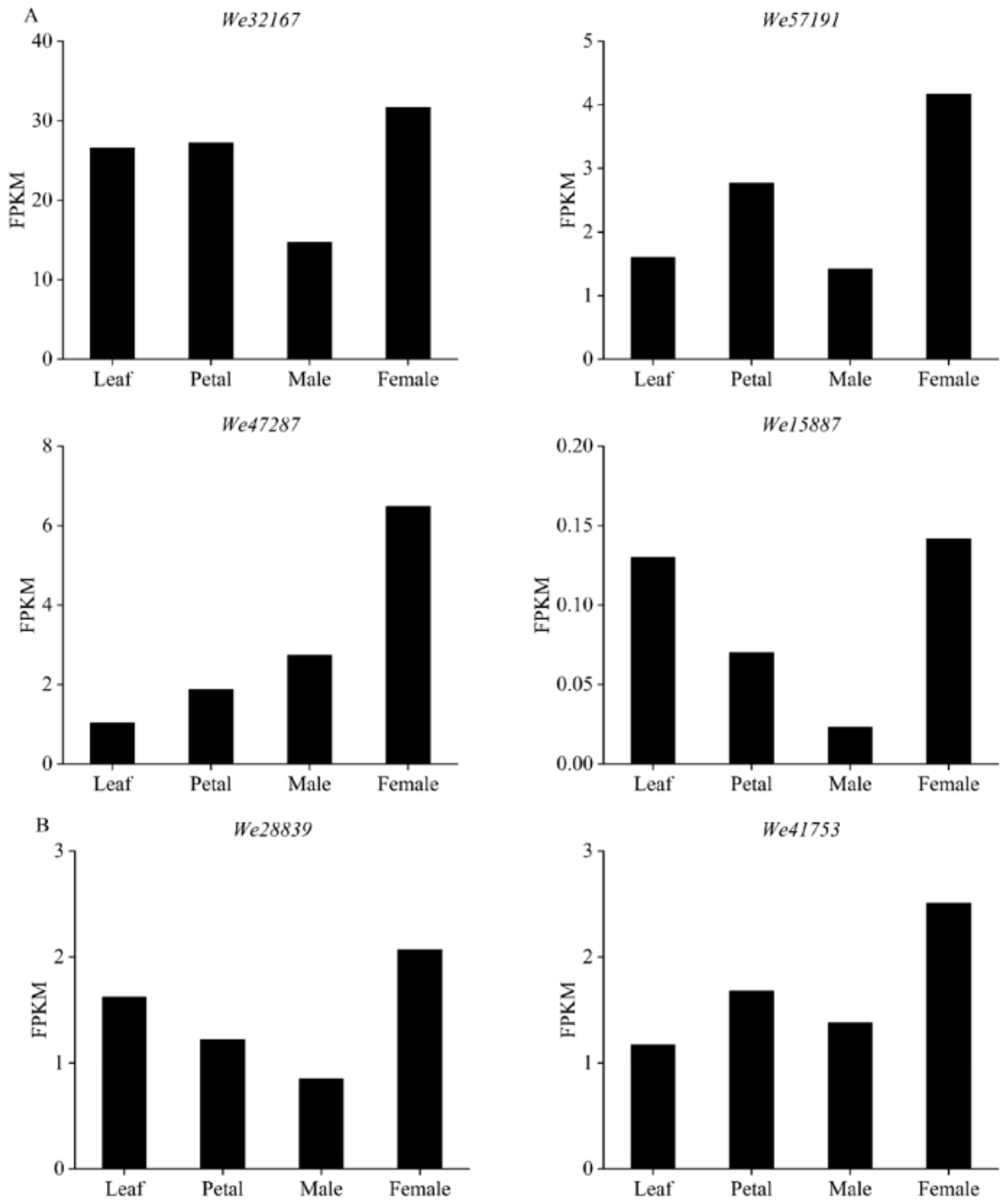

Figure 8

Non-tissue-specific expression of SRNL and SLFL (partial) (A) Non-tissue-specific expression of pollen S genes in *C.pilosula*. (B) Non-tissue-specific expression of style S genes in *C.pilosula*

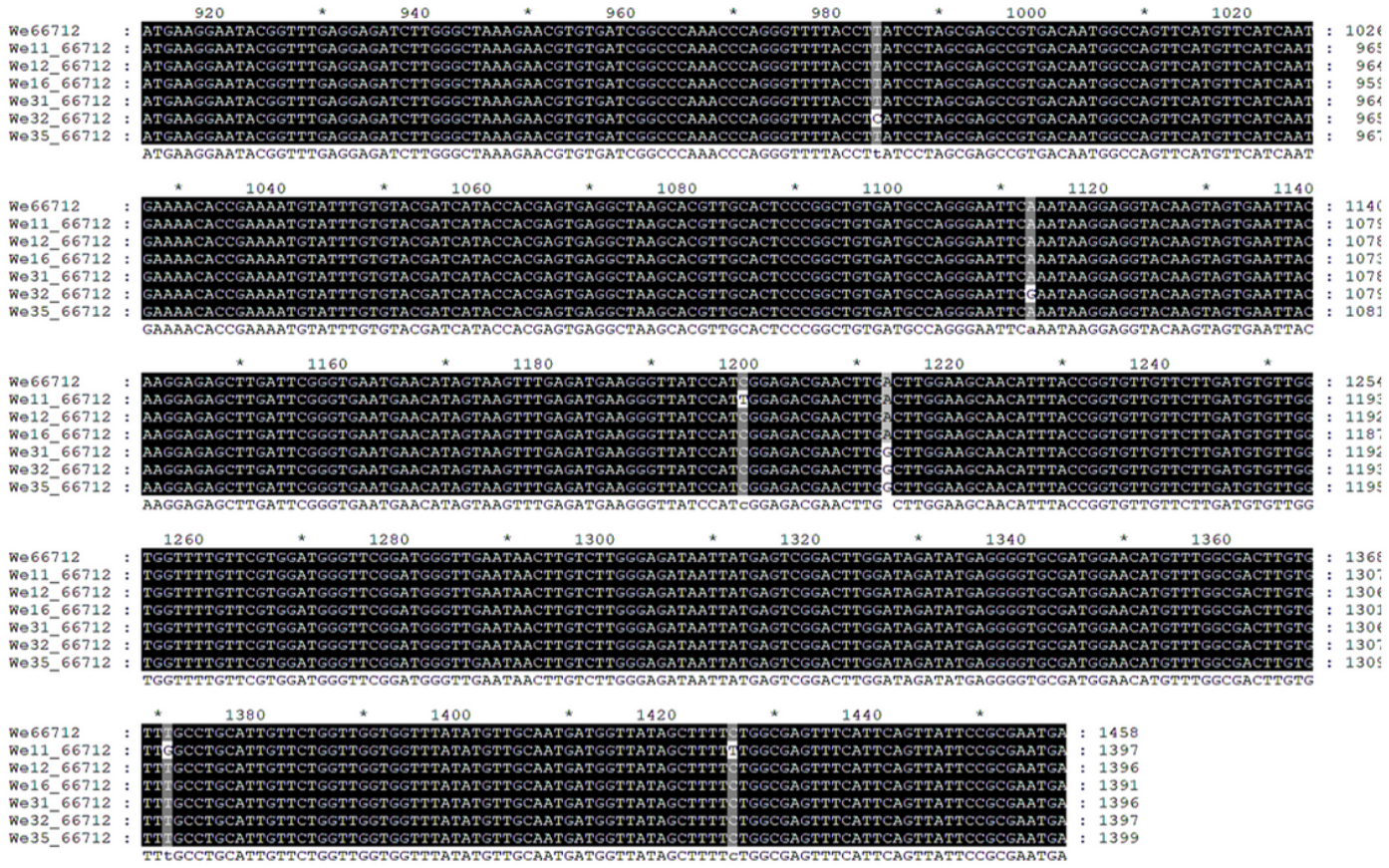

Figure 9

Sequence of pollen S gene *We66712* (partial) We11_66712; We12_66712; We16_66712; We31_66712; We32_66712; We35_66712 are Sanger sequencing of *We66712* gene in 'We'.